

# Core component EccB1 of the *Mycobacterium tuberculosis* type VII secretion system is a periplasmic ATPase

Xiao-Li Zhang,<sup>\*,†,‡,1</sup> De-Feng Li,<sup>†,1</sup> Joy Fleming,<sup>†</sup> Li-Wei Wang,<sup>†</sup> Ying Zhou,<sup>†</sup> Da-Cheng Wang,<sup>†</sup> Xian-En Zhang,<sup>\*,†,2</sup> and Li-Jun Bi<sup>†,2</sup>

<sup>\*</sup>State Key Laboratory of Virology, Wuhan Institute of Virology, Chinese Academy of Sciences, Wuhan, China; <sup>†</sup>National Laboratory of Biomacromolecules and Laboratory of RNA Biology, Institute of Biophysics, Chinese Academy of Sciences, Beijing, China; and <sup>‡</sup>Graduate School, Chinese Academy of Sciences, Beijing, China

**ABSTRACT** Pathogenic mycobacteria transport virulence factors across their complex cell wall *via* a type VII secretion system (T7SS)/early secreted antigenic target-6 of kDa secretion system (ESX). ESX conserved component (Ecc) B, a core component of the T7SS architecture, is predicted to be a membrane bound protein, but little is known about its structure and function. Here, we characterize EccB1, showing that it is an ATPase with no sequence or structural homology to other ATPases located in the cell envelope of *Mycobacterium tuberculosis* H37Rv. We obtained the crystal structure of an EccB1-ΔN72 truncated transmembrane helix and performed modeling and ATP docking studies, showing that EccB1 likely exists as a hexamer. Sequence alignment and ATPase activity determination of EccB1 homologues indicated the presence of 3 conserved motifs in the N- and C-terminals of EccB1-ΔN72 that assemble together between 2 membrane proximal domains of the EccB1-ΔN72 monomer. Models of the EccB1 hexamer show that 2 of the conserved motifs are involved in ATPase activity and form an ATP binding pocket located on the surface of 2 adjacent molecules. Our results suggest that EccB may act as the energy provider in the transport of T7SS virulence factors and may be involved in the formation of a channel across the mycomembrane.—Zhang, X.-L., Li, D.-F., Fleming, J., Wang, L.-W., Zhou, Y., Wang, D.-C., Zhang, X.-E., Bi, L.-J. Core component EccB1 of the *Mycobacterium tuberculosis* type VII secretion system is a periplasmic ATPase. *FASEB J.* 29, 4804–4814 (2015). [www.fasebj.org](http://www.fasebj.org)

**Key Words:** virulence • ESX-1 • crystal structure

*Mycobacterium tuberculosis* (MTB), the causative agent of tuberculosis, latently infects about one-third of the world's population, and deaths from active tuberculosis disease reached 1.5 million in 2013 (1). The success of bacterial pathogens depends on special protein export systems that secrete virulence factors into the extracellular milieu or inject them directly into host cells (2). Seven types of

secretion system have been identified, with types I–VI being distributed widely among gram-negative bacteria. As might be expected, MTB has a specialized secretion system due to its complex cell wall composition. The secretion system in MTB has been proposed as a novel ESAT-6 secretion system (ESX) or type VII secretion system (T7SS) (3, 4); however, its architecture and secretory mechanism are poorly understood. The T7SS can export ESX and PE-PPE family proteins, some of which contribute to virulence and granuloma formation, spread between cells, and escape from phagosomes (5–8). Understanding the T7SS will therefore be key to understanding mycobacterial pathogenesis, and should help to facilitate identification of novel drug targets and vaccine candidates (9, 10).

The T7SS was first identified in MTB and was later found in other mycolata species and gram-positive bacteria (11). MTB contains 5 T7SS systems (ESX-1 to 5) likely derived from gene duplication events (12), but to date, only the ESX-1, ESX-3, and ESX-5 clusters have been shown experimentally to encode functional secretory systems (13); the ESX-1 system has been shown to be involved in virulence (14), the ESX-3 system to be involved in iron acquisition (15), and the ESX-5 system to secrete PE and PPE proteins (16). These secretion systems share a number of highly conserved components [unified nomenclature: ESX-conserved component (Ecc)], EccA-E and mycosin-I protease, and, with the exception of EccA, which is located in the cytoplasm, these components are all predicted to be membrane-bound proteins (17). Although the architecture of these systems is largely uninvestigated, EccB, EccC, EccD, and EccE in the ESX-5 secretion system of *Mycobacterium marinum* have been shown to form a large ~1.5 MDa membrane complex (18). T7SS systems are proposed to share a common secretory mechanism; T7SS

<sup>1</sup> These authors contributed equally to this work.

<sup>2</sup> Correspondence: X.E.Z., State Key Laboratory of Virology, Wuhan Institute of Virology, Chinese Academy of Sciences, Wuhan 430071, China. E-mail: [zhangxe@sun5.ibp.ac.cn](mailto:zhangxe@sun5.ibp.ac.cn); L.-J.B., National Laboratory of Biomacromolecules and Laboratory of RNA Biology, Institute of Biophysics, Chinese Academy of Sciences, Beijing, 15 Datun Rd., Chaoyang District, Beijing 100101, China. E-mail: [blj@ibp.ac.cn](mailto:blj@ibp.ac.cn)  
doi: 10.1096/fj.15-270843

This article includes supplemental data. Please visit <http://www.fasebj.org> to obtain this information.

Abbreviations: CFP-10, culture filtrate protein-10 kDa; Ecc, early secreted antigenic target-6 of kDa secretion system conserved component; ESX, early secreted antigenic target-6 of kDa secretion system; IM, inner membrane; MTB, *Mycobacterium tuberculosis*; T7SS, type VII secretion system

substrates are recognized in the cytosol, targeted to the inner membrane (IM), and then transported across the mycobacterial cell envelope. The precise role of each T7SS component in the secretion mechanism requires further elucidation.

The best-studied T7SS, the ESX-1 secretion system, is responsible for the secretion of the important virulence factors ESAT-6 and culture filtrate protein-10 kDa (CFP-10). It is a major virulence determinant in MTB and is related to mycobacterial survival inside the host (6). The vaccine strain *Mycobacterium bovis* BCG lacks the region of the genome encoding the ESX-1 system and is attenuated (19), and an orthologous ESX-1 system is present in the avirulent saprophyte *Mycobacterium smegmatis*, where it is reported to be involved in conjugation (20). Studies of ESX-1 suggest that substrates ESAT-6 and CFP-10 form a heterodimer and are targeted to EccC by a secretion signal located in the C-terminal of CFP-10, then delivered across the IM via channel protein EccD (21). EccC shows homology to VirD4, a core component of the type IV secretion system (T4SS) and has ATPase activity, leading to the suggestion that it provides energy for transporting substrates through the channel (22). EccD has 11 predicted transmembrane domains and is highly hydrophobic; it has therefore been hypothesized to constitute the membrane pore through which substrates are transported, but there is no formal evidence for this (6). Although the biochemical characteristics and high-resolution structures of some ESX-1 substrates such as CFP-10/ESAT-6 and PE/PPE (proteins rich in proline-glutamate and proline-proline-glutamate residues), and individual components such as EccA, ESX-1 secretion-associated protein G, and MycP, have been obtained, the ESX-1 core components, including the EccB, EccC, EccD, and EccE proteins of ESX-1, are poorly understood at the biochemical and structural level (13).

EccB is present in all 5 ESX systems, and EccB1 has been shown to be essential for the secretion of virulence factors by the ESX-1 system (23). It is predicted to have a transmembrane region (24), but its biochemical characteristics and structure are largely unknown. Here, we report the biochemical and structural characterization of MTB EccB1, showing that it is an ATPase that is located in the periplasmic space. We determine the structure of the periplasmic region of EccB1 and perform modeling and ATP docking studies. Together with ATPase activity analysis of EccB1 mutants, results from these studies suggest that periplasmic EccB1 is likely a hexameric ATPase that forms a substrate transport channel and that its mechanism of action is powered by ATP hydrolysis. This study provides the first biochemical and structural characterization of a conserved T7SS core component and increases our understanding of how T7SSs transport substrates across the complex mycobacterial cell envelope.

## MATERIALS AND METHODS

### Strains, media, and culture conditions

MTB H37Rv strains were cultured at 37°C in Middlebrook 7H9 broth (Difco Laboratories, Detroit, MI, USA) supplemented with 0.5% glycerol, 10% albumin-dextrose-catalase and 0.05% Tween 80.

### Cloning and mutagenesis

EccB1 is encoded by gene Rv3869 in MTB and is predicted to contain an N-terminal transmembrane region (24). Here, we cloned the periplasmic region (residues 72–480), named EccB1- $\Delta$ N72, amplified by PCR from genomic DNA of the MTB H37Rv strain, into a modified pET-28a vector (pLW) encoding an N-terminal 6 $\times$ His tag followed by a 3C protease cleavage site. The following truncations of EccB1: EccB1- $\Delta$ N106 (residues 106–480), EccB1- $\Delta$ C448 (residues 72–448) and EccB1- $\Delta$ C463 (residues 72–463), and 2 homologues of EccB1 from MTB H37Rv (*M.tb*EccB5- $\Delta$ N80; encoded by Rv1782, residues 80–506) and *M. smegmatis*MC<sup>2</sup>155 (*Ms*EccB1- $\Delta$ N72; encoded by MSMEG\_0060, residues 72–479) were also constructed and cloned into the above pLW vector. We also constructed site-directed mutants based on plasmid pLW-EccB1- $\Delta$ N72 using Pyrobest DNA polymerase (TaKaRa, Beijing, China). Constructs with mutations at residues 150 and 102 were named C150S and R102A, respectively. All primers are listed in Supplemental Table 1 and all constructs were verified by sequencing.

### Recombinant protein production

Plasmids were expressed in the *Escherichia coli* BL21 (DE3) strain and purified following procedures described previously (25) with minor modifications. Cells were cultured to an OD 600 value of 0.8 in standard LB medium at 37°C and were then induced with 0.4 mM isopropyl  $\beta$ -D-1-thiogalactopyranoside for 16 h at 16°C. Cells were harvested by centrifugation and resuspended in lysis buffer containing 20 mM Tris pH 8.0, 500 mM NaCl, and 20 mM imidazole. The resuspended cells were lysed by sonication in lysis buffer followed by high-speed centrifugation. Supernatants were applied to Ni<sup>2+</sup>-affinity resin (Chelating Sepharose Fast Flow, GE Healthcare, Piscataway, NJ, USA) in Poly-Prep chromatography gravity columns (Bio-Rad, Hercules, CA, USA). After washing successively with lysis buffer containing different concentrations of imidazole (20 and 60 mM), the target protein was eluted with lysis buffer containing 300 mM imidazole, then further purified by ion-exchange using a HiTrap Q Sepharose FF column (GE Healthcare), eluting with a linear gradient of Tris buffer (pH 8.0) containing 1 M NaCl, and size-exclusion using a Superdex200 column (GE Healthcare) with buffer containing 20 mM Tris pH 7.5, 100 mM NaCl. Proteins in the peak at ~14 ml were collected and concentrated, quantitated using a BCA protein assay kit (Pierce Biotechnology, Rockford, IL, USA), and then stored at –80°C until required.

### Computational structure prediction

The EccB1 transmembrane segment was predicted using the tied mixture hidden Markov model (Tmhmm), v2.0 (26). Constructs were generated, in part guided by the Psi-blast based secondary structure prediction (Psipred) protein analysis server (27).

### Subcellular localization

MTB H37Rv cells harvested at midlogarithmic phase and washed 3 times in cold PBS were disrupted by bead beating using 0.1 mm silica spheres (MP Fastprep-24) in lysis buffer (PBS buffer containing 250 mM sucrose, 1 mM EDTA, and Protease Inhibitor Cocktail (Roche, Basel, Switzerland). Unbroken cells were removed by centrifugation and supernatants were filtered by passing through a 0.22  $\mu$ m membrane 3 times. The cell wall fraction was separated by ultracentrifugation for 1 h at 27,000 g and washed twice in PBS–250 mM sucrose. Supernatants were divided into cell membrane and cytosolic fractions by ultracentrifugation for 4 h at 100,000 g. Pellets were processed in the same way as

described above, and protein concentration was measured and aliquots were stored at  $-80^{\circ}\text{C}$ . Cleared lysates were resolved into cell wall fractions, cytoplasmic fractions, and membrane fractions according to a previously reported method (28, 29).

### Protease susceptibility of EccB1

Whole MTB H37Rv cells were treated with proteinase K according to a previously published method (28, 30), with the following modifications. Freshly prepared proteinase K (10 mg/ml) was added to whole cells from a 200 ml culture to final concentrations of 100, 200, and 400  $\mu\text{g}/\text{ml}$ , which were then incubated on ice for 45 min. Reactions were quenched by addition of protease inhibitor PMSF to a final concentration of 2 mM. After incubation on ice for 5 min and addition of 6 $\times$  SDS loading buffer, samples were heated at  $80^{\circ}\text{C}$  for 30 min then analyzed by SDS-PAGE and Western blotting.

### Antibody production and Western blotting

EccB1 antiserum was obtained by immunizing rabbits with purified recombinant EccB1- $\Delta\text{N}72$ . Samples were subjected to 12% SDS-PAGE before transferring to a nitrocellulose membrane. The nitrocellulose membrane was blocked in  $1\times$  phosphate buffered saline with Tween 20 with 5% (w/v) nonfat milk for 1 h at room temperature and then incubated overnight at  $4^{\circ}\text{C}$  with a 1:1000 dilution of EccB1 antiserum or 1:500 dilution of GroEL2 antibody. After washing the membrane 3 times with phosphate buffered saline with Tween 20, bound primary antibody was detected by incubating with a secondary horseradish peroxidase-linked anti-rabbit IgG (1:5000, GE Healthcare) and chemiluminescent substrate (enhanced chemiluminescence -plus substrate, GE Healthcare) according to the manufacturer's instructions.

### ATPase activity assays

Purified EccB1 (a gift from D.-C. W.), EccB1- $\Delta\text{N}72$ , homologues and mutants were incubated in 30  $\mu\text{l}$  of ATPase buffer (25 mM Tris pH 7.5, 100 mM NaCl, 5 mM  $\text{MgCl}_2$ ), unless otherwise indicated. Each reaction mixture contained 5  $\mu\text{l}$  ( $\gamma$ - $^{32}\text{P}$ ) ATP (Perkin Elmer, Waltham, MA, USA) diluted 1000 times with 100  $\mu\text{M}$  ATP. Reactions were incubated at  $37^{\circ}\text{C}$  for 30 min then stopped by addition of 40  $\mu\text{l}$  buffer containing 0.5 M  $\text{H}_2\text{SO}_4$  and 1.5 mM  $\text{NaH}_2\text{PO}_4$ . 10  $\mu\text{l}$  200 mM  $\text{Na}_2\text{MoO}_4$  and 100  $\mu\text{l}$  *n*-butanol saturated with water were then added and vortexed for 1 min. The mixture was separated by centrifugation at 12,000 rpm for 2 min, and 50  $\mu\text{l}$  of the organic phase (containing  $\gamma$ - $^{32}\text{P}$ ) was added to 2 ml liquid scintillation liquid 440 and vortexed. The amount of radioactivity present in the mixture was determined by liquid scintillation counting (31, 32). All experiments were performed in triplicate.

### Differential scanning fluorometry

Differential scanning fluorometry was performed according to a previously published method (33). The reaction mixture contained 0.2 mg/ml proteins, Sypro Orange (S6650; Invitrogen, Carlsbad, CA, USA) diluted  $\times 500$ , and small molecule substrates ADP, ATP, and ATP- $\gamma$ -S (Sigma-Aldrich, St. Louis, MO, USA) at a final concentration of 2 mM in buffer containing 20 mM Tris-HCl pH 7.5 and 100 mM NaCl. Assays (25  $\mu\text{l}$  assay volume) were performed in an RT-PCR system (Bio-Rad CFX96, Bio-Rad, Hercules, CA, USA) (excitation, 488 nm; emission, 620 nm).

### Crystallization and structure determination

Native protein crystals were grown at  $16^{\circ}\text{C}$  using the hanging drop vapor diffusion method; 2  $\mu\text{l}$  drops contained 4 mg/ml

EccB1- $\Delta\text{N}72$  and reservoir solution (20 mM Tris pH 7.5, 100 mM magnesium formate, and 15% [w/v] polyethylene glycol 3350) in a 1:1 ratio. SeMet-EccB1- $\Delta\text{N}72$  proteins were purified and crystallized in the same way as native proteins, except for the addition of 1 mM DTT (34) during the protein purification process. All crystals were harvested and soaked in a cryoprotectant solution consisting of the crystallization condition supplemented with 10% (v/v) glycerol for several seconds, and then flash-cooled in liquid nitrogen. Diffraction data sets were collected on beam line BL17U at the Shanghai Synchrotron Radiation Facility. All data sets were processed using Mosflm. The initial phases were calculated using the PHENIX package (35). Residues in 1 asymmetric unit were automatically built using the Autobuild program and the initial model was traced manually using the Coot program (36). Structure refinement was performed with Phenix refine and the stereochemical quality of the refined structures was verified with Procheck (37). All structural representations were prepared with PyMol (DeLano Scientific, Palo Alto, CA, USA).

### BS<sup>3</sup> crosslinking

Purified EccB1 (a gift from D.-C.W.) was incubated in 20  $\mu\text{l}$  PBS buffer (137 mM NaCl, 27 mM KCl, 10.1 mM  $\text{Na}_2\text{HPO}_4$ , and 1.8 mM  $\text{KH}_2\text{PO}_4$ , pH 7.4). Each reaction mixture contained 8  $\mu\text{M}$  EccB1 and BS<sup>3</sup> at different concentrations [0 (control), 0.375, 1.25, and 3.75 mM]. Reactions were incubated at  $22^{\circ}\text{C}$  for 30 min before adding 1  $\mu\text{l}$  1 M Tris, pH 7.5 and incubating at room temperature for 15 min to quench the reaction. The migration of protein bands was examined on 8% SDS-PAGE gels.

### Dynamic light scattering

The hydrodynamic diameter of EccB1- $\Delta\text{N}72$  was measured at  $25^{\circ}\text{C}$  using dynamic light scattering (Nanostar; Malvern Instruments, Malvern, United Kingdom). A 2.0 mg/ml solution of EccB1- $\Delta\text{N}72$  in 20 mM Tris, pH = 7.5, 100 mM NaCl, with or without the addition of 0.5 mM ATP was used. An average of 10 successive measurements was made at 1-min intervals.

### Accession codes

PDB coordinates and structure factors from the 2 structures were deposited in the Protein Data Bank archive with accession codes 3X3M and 3X3N.

### Modeling of EccB1

Modeling of the EccB1 hexamer was performed using the SymmDock web server (38). The 20 EccB1 hexamer models with the highest geometric shape complementarity scores were generated, and the 5 models with the largest complex approximate interface area and atomic contact energy were chosen. All 5 models had the same hexamer oligomerization state, but showed subtle differences in the complex interface. The model with the highest score was thus chosen as the model of EccB1. An ATP molecule was docked into the EccB1 structure using PatchDock (39). The 20 ATP-docked EccB1 models with the highest geometric shape complementarity scores were generated. These models showed some differences in the binding surface for ATP, and 3 of the models suggested that ATP binds close to conserved motifs 1 and 2 but had very slight differences in the ATP contact residues. We thus chose the model with the highest score to represent the ATP-binding model. After both the EccB1 hexamer and the EccB1-ATP complex were modeled, a total of 6 ATP

molecules were modeled into the EccB1 hexamer manually to create an ATP-bound EccB1 hexamer.

## RESULTS

### EccB1 localizes to the mycobacterial cell envelope

EccB1, encoded by gene Rv3869, is essential for ESX-1-dependent secretion and has been predicted to reside in the periplasmic space (24). Recently, Houben *et al.* reported that EccB5, the *M. marinum* homologue of EccB1, along with EccC5, EccD5, and EccE5 form a membrane complex in the cell envelope of *M. marinum*, suggesting that these components may form a translocation channel in the mycobacterial cell envelope (13). To provide experimental evidence of the subcellular location of EccB1 in MTB, we fractionated MTB H37Rv cells into the cell cytoplasm, cell membrane, and cell wall fractions, and then verified the location of EccB1 in these fractions using Western blotting with a set of specific antibodies (anti-GroEL2, and anti-EccB1-ΔN72). EccB1 mainly localized to the cell envelope fraction, consisting of both the IM and the mycolic-acid containing cell wall (Fig. 1A), consistent with the prediction that EccB1 is a periplasmic protein with an N-terminal transmembrane region. We also investigated the susceptibility of native EccB1 to proteases to confirm its location. Protease treatment of whole cells with 200 or 400 μg/ml proteinase K led to an obvious reduction in the quantity of EccB1, while no detectable reduction was found in the GroEL2 control (Fig. 1B). As EccB1 is not intrinsically resistant to protease K, this result implies that EccB1 resides predominantly outside the IM of the cell, in agreement with results from the cell fractionation experiment. Taken together, these findings indicate that EccB1 resides at the cell envelope of MTB.

### EccB1 is an Mg<sup>2+</sup>-dependent ATPase

As EccB3, a homologue of EccB1, is predicted to contain an ATP binding motif in its C-terminal, we investigated the ability of EccB1 to hydrolyze ATP using a radioactive assay with (γ-[<sup>32</sup>P]) ATP as the substrate. The kinetic parameters  $K_m$ ,  $V_{max}$ , and  $k_{cat}$  for ATP, calculated according to the Michaelis-Menten equation (Fig. 2A), demonstrate that EccB1 is indeed an intrinsic ATPase, its kinetic parameters ( $K_m$ :  $94.94 \pm 9.3 \mu\text{M}$ ;  $V_{max}$ :  $2.27 \pm 0.082 \mu\text{M}/\text{min}$ ;  $k_{cat}$ :  $0.76 \pm 0.012 \text{ min}^{-1}$ ; and  $k_{cat}/K_m$ :  $0.48 \mu\text{M}^{-1} \text{ s}^{-1}$ ) being in the same order of magnitude as values reported for EccA (Rv3868) (40). As we were unable to obtain sufficient quantities of full-length EccB1 to perform additional biochemical studies, we designed an N-terminal-truncated EccB1 construct (EccB1-ΔN72, residues G72-P480) based on analysis of the transmembrane region using protein analysis server Tmhmm v2.0 (26) and secondary structural stability using Psipred (27) in order to further characterize the ATPase activity of EccB1. Although the ATPase activity of EccB1-ΔN72 was significantly lower than that of full-length EccB1, its activity was still evident ( $K_m$ :  $9.87 \pm 1.64 \mu\text{M}$ ;  $V_{max}$ :  $0.09 \pm 0.004 \mu\text{M}/\text{min}$ ,  $k_{cat}$ :  $0.011 \pm 0.0002 \text{ min}^{-1}$  and  $k_{cat}/K_m$ :  $0.067 \mu\text{M}^{-1} \text{ s}^{-1}$ ) (Fig. 2B). We next investigated the effect of Ca<sup>2+</sup> and Mg<sup>2+</sup> ions on its ATPase

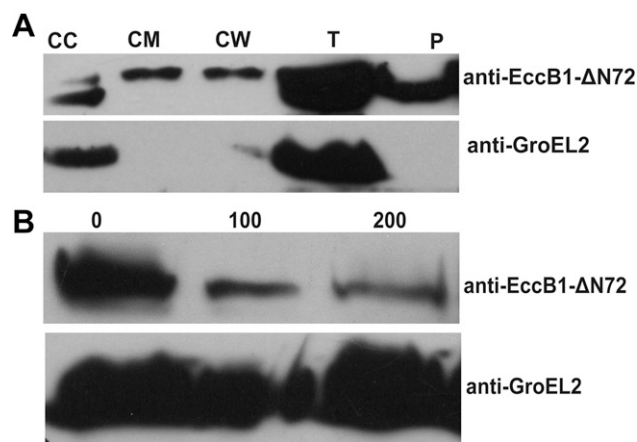


**Figure 1.** EccB1 localizes to the mycobacterial cell envelope. A) Immunoblot of different cell fractions: cell cytoplasm (CC), cell membrane (CM), and cell wall (CW) fractions, total protein (T), and EccB1-ΔN72 recombinant protein (P), using antibodies against EccB1-ΔN72 or GroEL2 (a cytoplasmic protein). B) Protease susceptibility of EccB1 at different concentrations of protease K. Whole cells were digested at protease concentrations of 0, 200, and 400 μg/ml. Immunoblotting was performed using antibodies against EccB1-ΔN72 and GroEL2.

activity. Addition of 5 mM EDTA abolished ATPase activity, but ATPase activity in the presence of 5 mM Mg<sup>2+</sup> was not significantly different from the native EccB1-ΔN72 control, and addition of 5 mM Ca<sup>2+</sup> reduced ATPase activity relative to the control (Fig. 2C). These results were independently corroborated by differential scanning fluorimetry in the presence of Ca<sup>2+</sup> and Mg<sup>2+</sup> ions, EDTA, AMP, ADP, ATP, and its analog ATP-γ-S. The addition of ATP, Mg<sup>2+</sup> ions, or a combination of both, led to an upward shift in the melting temperature of EccB1-ΔN72, but there was no change in the melting temperature on addition of EDTA, suggesting that the binding of ATP, or Mg<sup>2+</sup> ions improved the stability of EccB1-ΔN72. Addition of other components did not result in significant conformational transitions (Supplemental Fig. 1). Taken together, these results indicate that Mg<sup>2+</sup> ions are necessary for the ATPase activity of EccB1-ΔN72, and that EccB1-ΔN72 binds ATP but not the other molecules in the presence of Mg<sup>2+</sup>.

### ATPase activity is a common characteristic of EccB1 and its homologues

To determine whether ATPase activity is a feature of EccB1 homologues, we examined ATPase activity in EccB1 homologues from MTB and *M. smegmatis*. We cloned, expressed, and purified the periplasmic regions of MsEccB1 (MsEccB1-ΔN72 NT, encoded by MSMEG\_0060, residues 72–479) and MtEccB5 (MtEccB5-ΔN80, encoded by Rv1782, residues 80–506) and compared their ATPase activity with that of EccB1-ΔN72. MtEccB5-ΔN80 showed about 50% of the ATPase activity of EccB1-ΔN72, and a C-terminal 6xHis-tagged MsEccB1-ΔN72 CT had about 5 times the ATPase activity of EccB1-ΔN72. By contrast, an N-terminal 6xHis-tagged MsEccB1-ΔN72 NT lost its activity (Fig. 3). We conclude that ATPase activity is a common characteristic of these EccB1 homologues and likely involves the N-terminal, and we hypothesize that

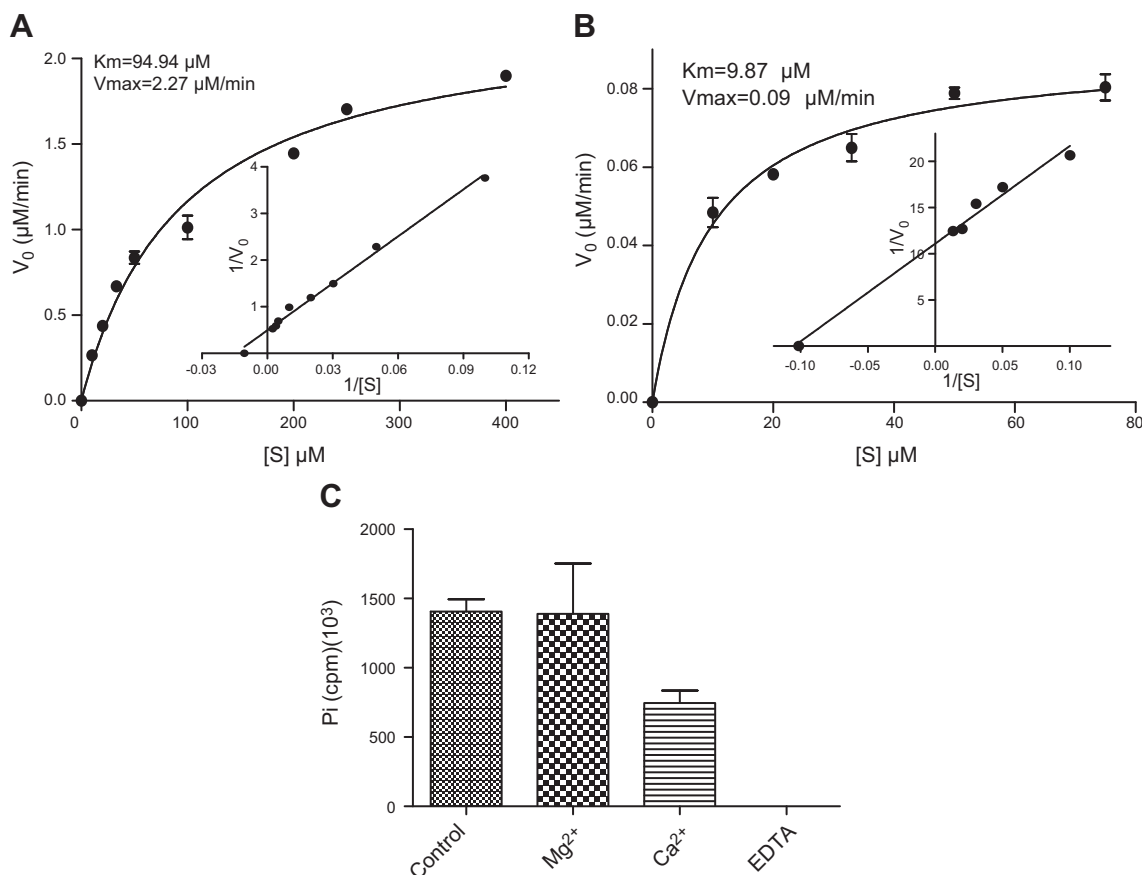


**Figure 2.** EccB1 is an Mg<sup>2+</sup> dependent ATPase. *A, B*) The kinetic parameters,  $K_m$  (Michaelis constant) and  $V_{\text{max}}$  of EccB1 (*A*) and EccB1- $\Delta\text{N72}$  (*B*) for ATP were measured by changing the concentrations of ATP at fixed concentrations of EccB1/EccB1- $\Delta\text{N72}$ . Kinetic parameters were calculated by fitting the data to the Michaelis-Menten equation. The insert shows a Lineweaver-Burk plot of  $K_m$  and  $V_{\text{max}}$ . *C*) Effect of Mg<sup>2+</sup>, Ca<sup>2+</sup>, and EDTA on ATPase activity. ATPase activity of EccB1 was measured in the presence and absence (control) of 5 mM Mg<sup>2+</sup>, Ca<sup>2+</sup>, and EDTA. Addition of Ca<sup>2+</sup> led to a 50% decrease in ATPase activity and addition of EDTA abrogated ATPase activity. Addition of Mg<sup>2+</sup> had no significant effect on ATPase activity. Results presented are from 3 replicate experiments.

this ATPase activity may play a key role in providing the energy required for transport of virulence factors in the type VII secretion system.

### Two conserved sequence motifs, located in the N- and C-terminals, and important residues are involved in ATPase activity

We next compared the sequences of EccB1 and its homologues to identify any conserved sequence motifs that might be involved in its ATPase activity. Sequence alignment identified 3 conserved motifs: residues 94–103 (motif 1, PX<sub>2</sub>NLXSARL), residues 125–134 (motif 2, GX<sub>2</sub>hGIPGAP; h indicates hydrophobic residues) and residues 429–463 [motif 3, LGLX<sub>5-7</sub> (A/I) PWX<sub>2</sub>HX<sub>2</sub> (L/F) X<sub>2</sub>GPXLSX<sub>3</sub>AXhX<sub>2</sub>DXh] (Fig. 4). Motifs 1 and 2 are located at the N-terminal of the periplasmic region and motif 3 at the C-terminal. To verify the effect of conserved motifs on ATPase activity, we examined the ATPase activity of 3 truncations (Fig. 4B). Deletion of motif 1 (EccB1- $\Delta\text{N106}$ , residues 106–480) totally abolished ATPase activity and deletion of different numbers of residues of the C-terminal of EccB1 (EccB1- $\Delta\text{C448}$

and EccB1- $\Delta\text{C463}$ , corresponding to residues 72–448 and 72–463, respectively) increased ATPase activity. These results indicate that motif 1 is directly involved in ATPase activity and that the C-terminal of EccB1, including motif 3, also affects ATPase activity. As we were unable to obtain a truncation in which motif 2 was deleted, we were not able to determine whether motif 2 is involved in ATPase activity. However, the rich composition of proline and glycine residues in motif 2 leads us to suggest that it might be involved in stabilizing local protein conformation.

We subsequently performed mutagenesis studies on 2 conserved residues likely to be of significance in EccB1 activity. Residue Arg102 of conserved motif 1 is notable in that it is the only charged residue in this motif. Mutation of this residue to alanine significantly decreased the ATPase activity of EccB1- $\Delta\text{N72}$ , indicating that it is likely involved in ATPase activity (Fig. 4C). Sequence analysis suggests that residues Cys150 and Cys345 may form a disulfide bond. Mutation of residue Cys150 to serine likely destroys this, the only disulfide bond within EccB1, and thus the overall folding of the protein. Mutant C150S lost most of its ATPase activity (Fig. 4C), confirming that a stable structure is important for ATPase activity.

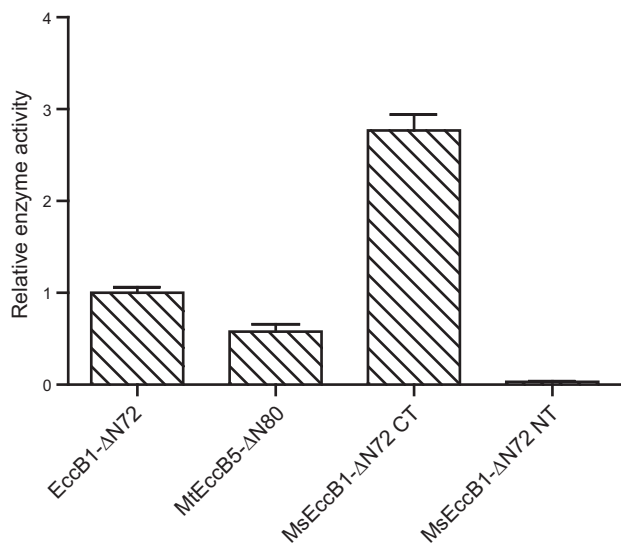


**Figure 3.** ATPase activity is a common characteristic of EccB1 and its homologues. Recombinant proteins EccB1-ΔN72, MtEccB5-ΔN80 (encoded by Rv1782), and MsEccB1-ΔN72 NT (encoded by MSMEG\_0060) with N-terminal His tags and MsEccB1-ΔN72 CT with a C-terminal His tag were incubated with ( $\gamma$ -[ $^{32}$ P]) ATP at 37°C. The hydrolytic activity of EccB1-ΔN72 was considered as 100%. MtEccB5-ΔN80 showed ~50% activity relative to EccB1-ΔN72, and MsEccB1-ΔN72 CT showed nearly 3 times the activity of EccB1-ΔN72. By contrast, MsEccB1-ΔN72 NT lost most of its ATP hydrolytic activity.

### The N- and C-terminals are located in close proximity within the crystal structure

To further investigate the catalytic sites involved in EccB1's ATPase activity, we determined the crystal structure of the periplasmic region of EccB1, EccB1-ΔN72, at 1.9 Å resolution. Crystallographic parameters are summarized in **Table 1**. Initial phases were derived from a single wavelength anomalous dispersion experiment using a SeMet-substituted protein. The model comprises 393 residues, including EccB1 residues Gly72 to Ala465 and 3 residues from the vector. One asymmetric unit contains a single protein molecule. Fifteen residues are missing at the C-terminal of the model due to the flexibility of the protein sequence making interpretation impossible. The overall structure of EccB1 comprises 5 domains, referred to as domains A1 (residues 72–135), B1 (one half of domain B, residues 143–180), C1 (residues 181–242), A2 (residues 265–323), B2 (the other half of domain B, residues 342–390), and C2 (residues 391–451) (**Fig. 5**). These domains are arranged in an “S”-like line in the order A1-C2-B1-B2-C1-A2 from membrane-proximal to membrane-distal. Domains A1, C1, A2, and C2 fold in the same  $\alpha/\beta/\alpha$  sandwich fold and have a common core consisting of a 3-stranded  $\beta$ -sheet sandwiched between 2  $\alpha$ -helices. The domains vary in the presence or absence or additional  $\beta$ -strands that are connected with the  $\alpha$ -helices, giving a secondary structure arrangement of  $\beta$ - $\beta$ - $\alpha$ - $\beta$ /loop- $\alpha$ - $\beta$ /loop. Subdomains B1 and B2 both fold into similar 3  $\beta$ -stranded motifs, and are connected via a disulfide bond between residues Cys150 and Cys345 to form an intact 6-stranded  $\beta$ -sheet with a pseudo 2-folded symmetric axis. The sequences and structures of domains A1, B1, and C1

are similar to those of domains A2, B2, and C2, giving the overall structure of EccB1 a pseudo-2-folded axis of symmetry via the pseudo-2-folded symmetric axis observed in domain B. The 3 conserved motifs involved in the ATPase activity are located at the interface of membrane-proximal domains A1 and C2 and are in close proximity. The structure suggests that destruction of the only disulfide bond in EccB1 (Cys150-Cys345) may destroy the overall folding of the protein by disrupting the overall integrity of the B domain, in turn leading to the disruption of the interface of domains A1 and C2. This may explain why mutation of Cys150 to Ser leads to the loss of most of the ATPase activity of EccB1-ΔN72 (**Fig. 4C**).

### ATP-binding pockets are formed by the N- and C- terminal conserved motifs from adjacent EccB1 molecules within a proposed hexamer arrangement

Size-exclusion chromatography and BS<sup>3</sup> crosslinking results confirmed that EccB1 may form an oligomer (**Supplemental Fig. 3**). Dynamic light scattering also indicated that EccB1-ΔN72 likely forms an oligomer on addition of ATP (**Supplemental Fig. 3**). As most ATPases identified in other secretion systems function as hexamers and the EccBCDE complex identified in *M. marinum* contains 6 copies of EccB (18), we hypothesized that EccB1 forms a hexamer to fulfill its biologic function in the T7SS. We thus modeled a 6-fold rotational symmetric EccB1 oligomer using the SymmDock Web server and then docked the ATP molecule into the EccB1 hexamer according to the method described above. The hexamer of EccB1 has the appearance of an hourglass shaped channel with 2 large pores, 1 formed by domain A2 close to the mycolic membrane and the other by domain A1 close to the IM, and 1 small pore formed by domain C2 in the middle (**Fig. 6A**). The diameter of the small pore is about 20 Å and is comparable in diameter to the ESXA/B heterodimer (~22 Å) and DNA duplexes (~20 Å), 2 potential substrates of T7SS. In this model, the ATP molecule resides at the interface of 2 subunits, at the same vertical latitude as the small pore. The ATP molecule is surrounded by motif 3A (LGLX<sub>5-7</sub> [A/I] PW) and motif 1 from 1 EccB1 protomer and motif 3B (X<sub>2</sub>HX<sub>2</sub> [L/F] X<sub>2</sub>GPXLSX<sub>3</sub>AXhX<sub>2</sub>DXh) from an adjacent protomer. These 2 conserved sequence motifs together thus comprise the ATP binding pocket (**Fig. 6B**). This observation supports our proposal that EccB1 forms a hexamer. We further propose that T7SS substrates may be secreted outside of the mycolic membrane from the periplasm via EccB1 or its homologous hexamers.

## DISCUSSION

The biochemical and structural characteristics of EccB1, a core component of the ESX-1 system that is essential for its secretion of virulence factors, are largely unknown (6). Here, we demonstrate that EccB1 is an ATPase located in the periplasmic space of MTB. We solved the structure of the periplasmic region of EccB1, and these data, together with that from ATP docking studies with an EccB1 hexamer oligomer model and ATPase activity analysis of EccB1 mutants, suggest that periplasmic hexameric ATPase EccB1

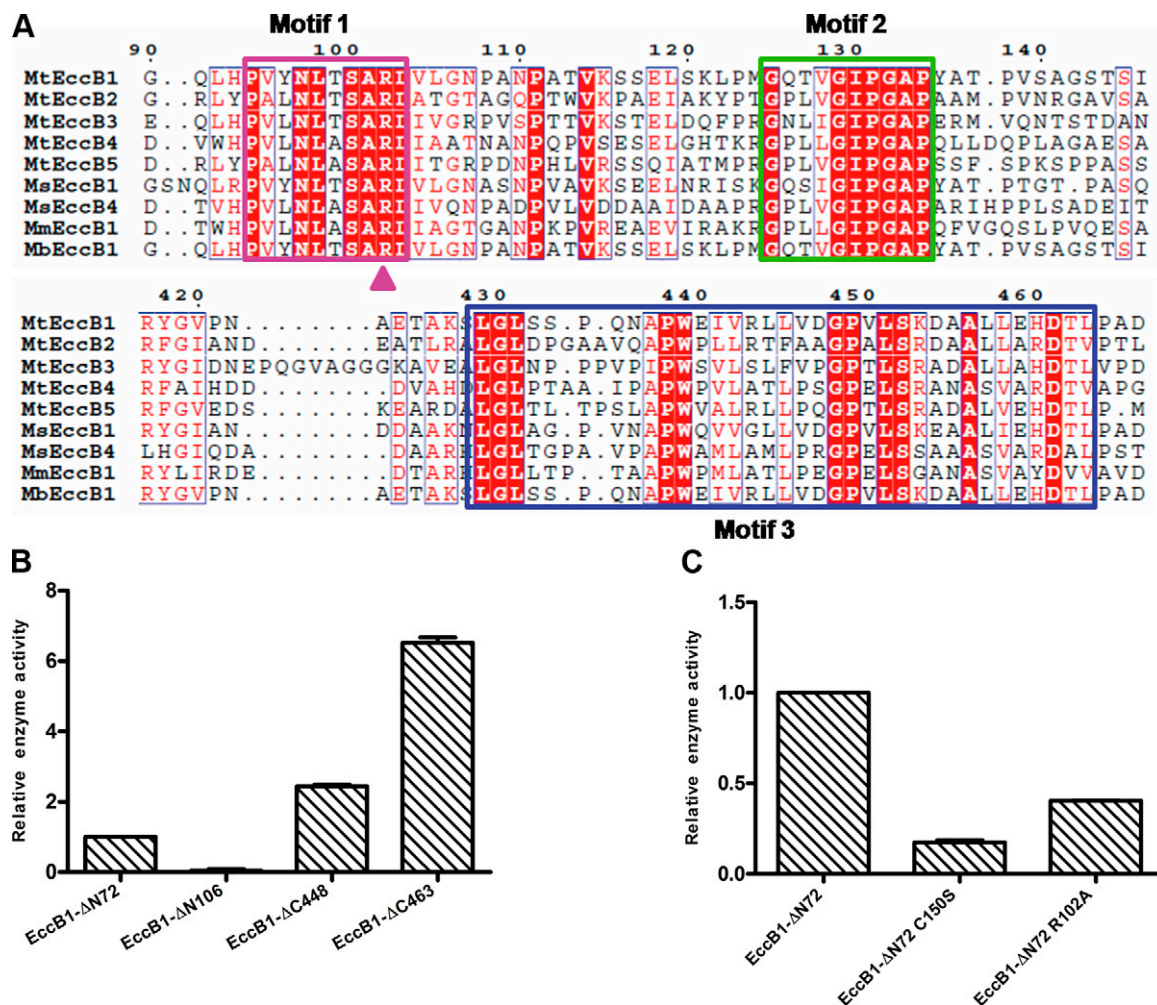


**Figure 4.** Conserved sequence motifs, located in both the N- and C- terminals of EccB1, are involved in its ATPase activity. **A**) Comparison of the amino acid sequence of MtEccB1 with MtEccB5, MsEccB1, MsEccB4, MmEccB1, and MbEccB1. *M. tuberculosis* (Mt), *M. smegmatis* (Ms), *M. marinum* (Mm), and *M. bovis* (Mb) revealed 3 conserved motifs. Motif 1 (residues 94–103), motif 2 (residues 125–134), and motif 3 (residues 429–463) are indicated by magenta, green, and blue boxes, respectively, and the conserved residue Arg 102 by a magenta triangle. Motifs 1 and 2 are localized at the N-terminal of EccB, and motif 3 at the C-terminal. **B**) ATPase activity of different truncations and mutants of EccB1. The ATPase activity of 3 EccB1-ΔN72 truncations designed based on sequence analysis, EccB1-ΔN106 (deletion of motif 1), EccB1-ΔC448 (deletion of residues 449–480 of motif 3) and EccB1-ΔC463 (deletion of residues 463–480) was detected. The ATPase activity of EccB1-ΔN72 was considered as 100%. EccB1-ΔN106 had almost no activity, while the activity of EccB1-ΔC448 and EccB1-ΔC463 increased by 2 and 6 times, respectively. **C**) The ATPase activity of EccB1-ΔN72 mutants Arg102 to Ala (R102A) and Cys150 to Ser (C150S) decreased relative to EccB1-ΔN72, retaining 40 and 20% activity, respectively. Results presented are the means of 3 replicate experiments.

forms a substrate transport channel and that the mechanism of transport across the complex mycomembrane may be powered by ATP hydrolysis.

Houben *et al.* recently reported that EccB5, an EccB1 homologue, is located in the cell envelope of *M. marinum*, where it forms a large membrane complex along with EccC5, EccD5, and EccE5 (18). The mycobacterial cell envelope is highly complex and is composed of the plasma membrane, the cell wall, which is comprised of peptidoglycan, arabinogalactan, the mycomembrane, which is mainly comprised of long chain (C60–C90) mycolic fatty acids, and an outermost layer known as the capsule (41, 42). In line with Houben *et al.*, results here show that EccB1 is present in both the plasma membrane and cell wall fractions of MTB (Fig. 1A) and further indicate that EccB1 resides outside the plasma membrane (Fig. 1B), indicating

that it is a periplasmic protein. Generally speaking, secretion system proteins located in the periplasmic space are involved in the formation of transport channels across the outer membrane, or packaging substrates. For this reason, we hypothesized that EccB1, like its EccB5 homologue, may be involved in the formation of a channel spanning both the plasma membrane and mycomembrane.

The T7SS possesses a powerful army of energy-producing molecules, including at least 2 known ATPases: EccA and EccC (12). EccB proteins have not previously been shown to have ATPase activity. EccB1 has low sequence homology with known ATPases, and lacks the Walker A motif, also referred to as a phosphate-binding (P) loop (GX<sub>4</sub>GK [T/S]), present in most ATPases (Supplemental Fig. 2). Our study demonstrates that the ATP binding motif of EccB1 is different from those previously reported.

TABLE 1. *Crystallographic statistics*

Crystals	EccB1-ΔN72	SeMet-EccB1-ΔN72
Data collection		
Space group	P212121	P21
Cell dimensions		
<i>a</i> , <i>b</i> , <i>c</i> (Å)	31.63, 108.73, 114.53	31.84, 122.65, 60.42
$\alpha$ , $\beta$ , $\gamma$ (deg)	90, 90, 90	90, 101.27, 90
Wavelength (Å)	1.5418	0.9789
Resolution (Å)	36.02–1.90 (2.00–1.90)	33.65–2.00 (2.11–2.00)
$R_{\text{merge}}^a$ (%)	5.6 (22.7)	10.1 (46.9)
$\langle I/\sigma \rangle$ (I)	9.9 (5.4)	12.3 (4.5)
Completeness (%)	97.0 (84.1)	98.4 (98.3)
Redundancy	6.1 (4.1)	9.1 (8.9)
Wilson plot B	18.5	33.1
Refinement		
Reflections ( <i>n</i> )	31,051	30,094
$R_{\text{work}}/R_{\text{free}}^+$ (%)	18.4 (22.5)	20.9 (24.0)
R.m.s.d.		
Bond lengths (Å)	0.004	0.006
Bond angles (deg)	0.936	1.051
Non-H atoms ( <i>n</i> )		
Total	3450	2979
Protein	2960	2851
Ligand/ion	2	2
Water	488	126
Average B factors (Å <sup>2</sup> )		
Total	24.5	58
Protein	22.9	58.3
Ligand/ion	31.5	67.5
Water	33.6	51.3
Ramachandran plot, residues (%)		
Favored	98.48	95.79
Allowed	1.01	3.16
Outliers	0.51	1.05

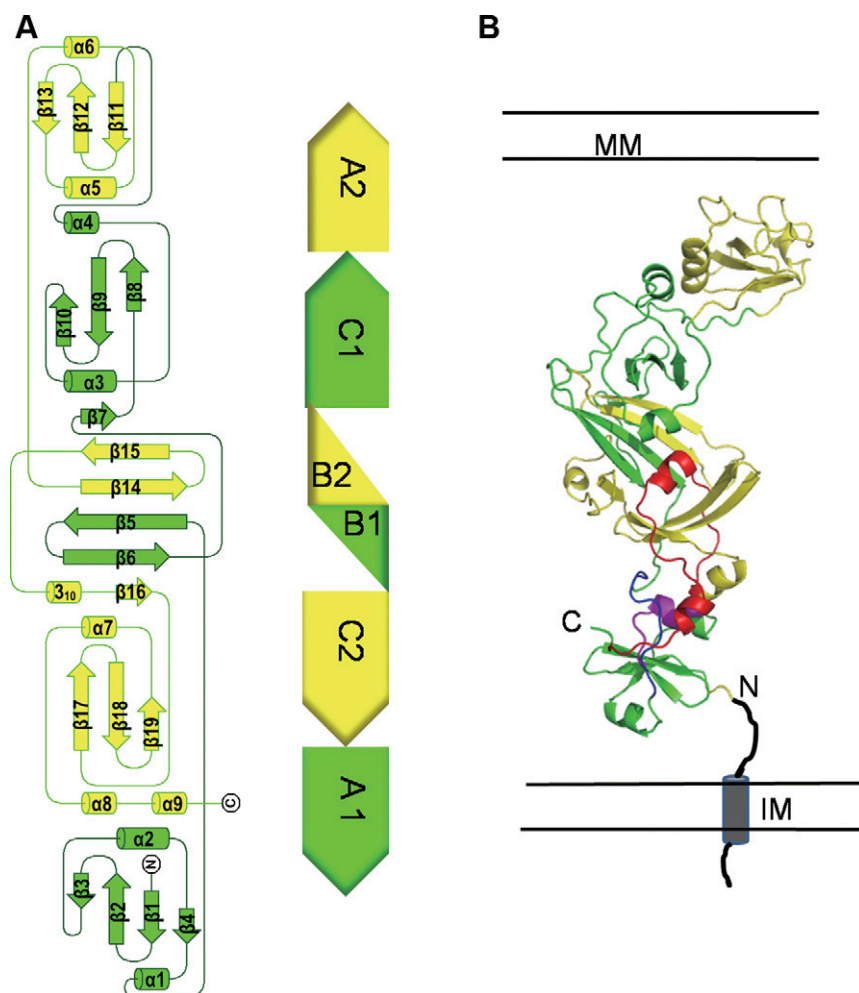
Values in parentheses are for the highest resolution shell.  $R_{\text{merge}} = \sum hkl \sum i |I_i(hkl) - \langle I(hkl) \rangle| / \sum hkl \sum i I_i(hkl)$ , where  $I_i(hkl)$  is the intensity of the *i*th measurement of reflection *hkl*.  $\sum i$  is the sum over the individual measurements of a reflection, and  $\sum hkl$  is the sum over all reflections. R.m.s.d., root-mean-square deviation;  $\langle I/\sigma \rangle$  (I), intensity over intensity of  $\sigma$ .

Sequence analysis indicated that there are 3 conserved motifs in the EccB1 sequence (Supplemental Fig. 2). ATPase activity determination of the truncation EccB1-ΔN106 indicated that the Walker A motif is likely functionally substituted by motif 1 which, like the Walker A motif, contains a conserved Arg102 residue (Fig. 4). Different from members of the secretion ATPase superfamily, such as VirB11, VirD4, and VirB4 of the T4SS in *Agrobacterium tumefaciens*, in which N-terminal and C-terminal domains are clearly separated (43), EccB1 is comprised of 5 domains in the arrangement A1-B1-C1-A2-B2-C2, which interweave and fold back on themselves to form a novel 3-D structure in which the domains are arranged in the order A1-C2-B1 and B2-C1-A2 along a pseudo-2-folded symmetric axis (Fig. 5). Size-exclusion chromatography and BS<sup>3</sup> crosslinking results showed that EccB1 may form an oligomer (Supplemental Fig. 3) and modeling of EccB1 to further investigate the features of its ATPase activity indicated that a hexamer arrangement gave the highest geometric shape complementarity scores. This is in line with the fact that many members of the secretion ATPase family exist as hexamers (43, 44). NanoLC-MS/MS analysis of the large T7SS membrane bound complex, EccBCDE, reported by Houben *et al.* and discussed

above, also showed that it contains 6 copies of EccB (18). ATP docking showed that the ATP binding pocket is located at the interface between 2 adjacent molecules (between motif 3A and motif 1 from the same molecule and motif 3B from an adjacent molecule). This was further confirmed by ATPase activity determination of EccB1 truncations (Fig. 4B). Dynamic light scattering results also indicated the formation of an oligomeric form of EccB1-ΔN72 on addition of ATP (Supplemental Fig. 3). The diameter of the small pore of the EccB1 hourglass shaped hexamer is about 20 Å, similar to the central channel of the EccC homologue T4SS TrwB spherical hexamer (22 Å), which transports DNA or proteins across the IM (45). We thus conclude that the EccB hexamer may act as part of a transport channel to deliver substrates and that its transport mechanism may be powered by ATP hydrolysis.

Most ATPases of the secretion ATPase superfamily drive substrates across the IM by ATP dephosphorylation, converting chemical energy into biologic activity, and have all of their ATPase domains in the cytoplasm. EccB1's location in the periplasmic space suggests that it possibly functions as a motor that powers substrates across the mycomembrane of MTB. We predict that EccB needs the help of

**Figure 5.** The N- and C terminals are located in close proximity within the crystal structure of MTB EccB1- $\Delta$ N72. **A)** EccB1 is a membrane-bound protein with a predicted N-terminal transmembrane helix (gray cylinder) spanning the IM. The structure of EccB1- $\Delta$ N72 is composed of 6 domains, A1-C2-B1-B2-C1-A2, listed from the membrane proximal N-terminal. Topological structure of EccB1- $\Delta$ N72. The similarity of the protein sequence of the A1-B1-C1 and A2-B2-C2 regions leads to folding along the axis shown into a 2-folded rotation symmetrical structure, bringing the N-terminal and C-terminal into close proximity. **B)** Crystal structure of EccB1- $\Delta$ N72 displayed as a cartoon. Domains A1, B1, and C1 are shown in green and other domains are shown in yellow. The 3 conserved motifs are shown in magenta (motif 1), blue (motif 2), and red (motif 3). IM, inner membrane; MM, mycomembrane.



other proteins to transport substrates across the mycomembrane as we did not detect direct interactions between EccB1 and the ESXA/B complex in either ITC or SPR experiments, and such interactions have not previously been reported. Houben *et al.* have proposed 2 different models for the T7SS transport mechanism based on the composition of the EccBCDE membrane complex (18). Their 2-step model presumes that the EccBCDE membrane complex is located entirely within the IM and simply transports substrates from the cytoplasm across the IM. Another transport channel is required to complete transport from the periplasmic space across the mycomembrane. In their 1-step model, however, EccE acts a bridge between the channel formed by the EccBCD complex and a second channel in the mycomembrane, facilitating 1-step transport. Our study provides support for the 1-step model: proteinase K digestion suggests that the soluble segment of EccB1 protrudes into the periplasmic space of MTB. In addition, the EccB1- $\Delta$ N72 structure is  $\sim 10$  nM too short to span both the mycobacterial plasma membrane and mycomembrane ( $\sim 20$  nM) (41). EccB1 thus requires other components to form a transport channel across the mycomembrane, but can likely act as a bridge between these 2 membranes.

EccB is present in all 5 ESAT-6 gene clusters and is crucial for ESAT-6/CFP-10 secretion (6, 23). Although, as shown in this study, some EccB1 homologues also have

ATPase activity, we still lack direct experimental evidence that this ATPase activity is related to substrate secretion. Verifying the involvement of ATPase activity in substrate transport will require experiments showing that EccB1 deletion can be complemented by different EccB1 truncations and EccB1 mutants in which key residues are mutated. Furthermore, it will be important to determine the structure and biochemical characteristics of EccB1 in complex with the proteins it interacts with in the formation of the transport channel.

In summary, we have shown that EccB is a periplasmic ATPase and have identified a putative ATP binding pocket via oligomer modeling, ATP docking, and mutagenesis experiments. We propose that EccB1 exists as a hexamer and is involved in transporting substrates from the periplasm to the outside of the cell via hydrolyzing ATP. Our work provides the first biochemical and structural data on an individual core component of the T7SS membrane complex and increases our understanding of T7SS architecture. Virulence factor secretion systems are considered to be potential drug targets. As such, our characterization, molecular modeling, and mutational analysis of EccB1 may set the stage for the identification of novel inhibitors that can disrupt the export of critical tuberculosis virulence factors (10). The subcellular location of EccB1 in the periplasmic space may facilitate drug delivery, making it an attractive target. FJ

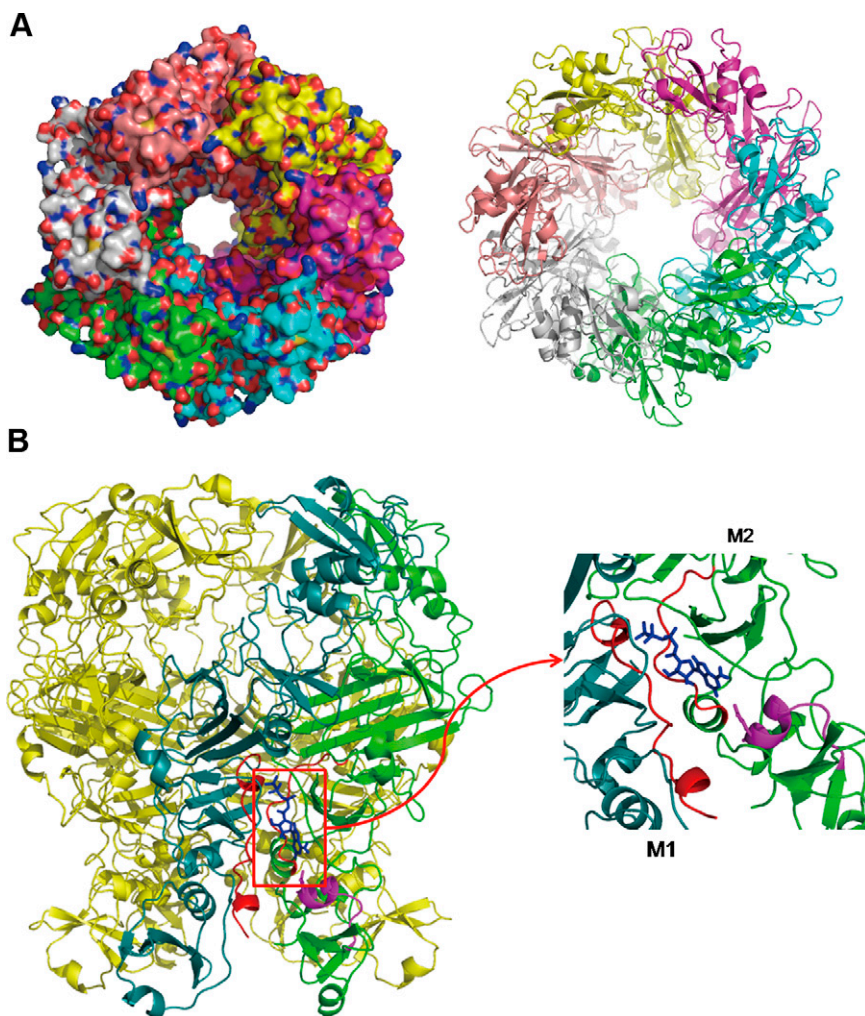


**Figure 6.** The N- and C- terminal conserved motifs from adjacent EccB1 molecules within a proposed hexamer arrangement form ATP-binding pockets. *A*) Top view of the molecular surface and cartoon of proposed 6-fold rotational symmetric oligomer of EccB1 as modeled by the SymmDock web server. The 6 molecules are indicated in different colors. *B*) An ATP molecule was docked into the EccB1 hexamer using Patch-Dock. The ATP molecule is shown as a stick model and is located at the interface between the molecules of 2 adjacent subunits. Enlargement of an ATP binding pocket in the EccB1 hexamer (red-boxed area). The pocket is formed from residues 440–458 of molecule M1 (motif 3B) and 429–439 of M2 (motif 1 and motif 3A). Mutation of motif 1 conserved residue Arg102, shown in red, decreases ATPase activity, providing support for this hexamer model.

The authors express their appreciation to the staff at the Shanghai Synchrotron Radiation Facility of China for assistance with collecting protein diffraction data, and thank Yi Han and Sheng-Quan Liu from the Institute of Biophysics, Chinese Academy of Sciences, for their assistance in data collection, Xiao-Xia Yu and Xiao-Qian Xie for assistance with protein purification, Hong-Jie Zhang and Wen-Jing Wei for help with the ATPase activity assay, and Hong-Tai Zhang for helpful discussions on the manuscript. This work was supported by grants from the National Basic Research Program of China (2011CB910300, 2012CB518700, 2013CB911500), the Key Project Specialized for Infectious Diseases of the Chinese Ministry of Health (2013ZX10003006 and 2012ZX10003002), the Chinese Academy of Sciences (KJZD-EW-L02, XDB08020200), and the National Natural Science Foundation of China (31170132, 31270792).

## REFERENCES

1. Eurosurveillance editorial team (2013) WHO publishes Global tuberculosis report 2013. *Euro Surveill.* **18**, 39
2. Finlay, B. B., and Falkow, S. (1997) Common themes in microbial pathogenicity revisited. *Microbiol. Mol. Biol. Rev.* **61**, 136–169
3. Bitter, W., Houben, E. N., Luirink, J., and Appelmek, B. J. (2009) Type VII secretion in mycobacteria: classification in line with cell envelope structure. *Trends Microbiol.* **17**, 337–338
4. Abdallah, A. M., Gey van Pittius, N. C., Champion, P. A. D., Cox, J., Luirink, J., Vandenbroucke-Grauls, C. M. J. E., Appelmek, B. J., and Bitter, W. (2007) Type VII secretion–mycobacteria show the way. *Nat. Rev. Microbiol.* **5**, 883–891
5. Abdallah, A. M., Savage, N. D. L., van Zon, M., Wilson, L., Vandenbroucke-Grauls, C. M. J. E., van der Wel, N. N., Ottenhoff, T. H. M., and Bitter, W. (2008) The ESX-5 secretion system of *Mycobacterium marinum* modulates the macrophage response. *J. Immunol.* **181**, 7166–7175
6. Stoop, E. J., Bitter, W., and van der Sar, A. M. (2012) Tubercle bacilli rely on a type VII army for pathogenicity. *Trends Microbiol.* **20**, 477–484
7. Van der Woude, A. D., Luirink, J., and Bitter, W. (2013) Getting across the cell envelope: mycobacterial protein secretion. *Curr. Top. Microbiol. Immunol.* **374**, 109–134
8. Van der Wel, N., Hava, D., Houben, D., Fluittsma, D., van Zon, M., Pierson, J., Brenner, M., and Peters, P. J. (2007) *M. tuberculosis* and *M. leprae* translocate from the phagolysosome to the cytosol in myeloid cells. *Cell* **129**, 1287–1298
9. Simeone, R., Bottai, D., and Brosch, R. (2009) ESX/type VII secretion systems and their role in host-pathogen interaction. *Curr. Opin. Microbiol.* **12**, 4–10
10. Bitter, W., and Kujil, C. (2014) Targeting bacterial virulence: the coming out of type VII secretion inhibitors. *Cell Host Microbe* **16**, 430–432
11. Pallen, M. J. (2002) The ESAT-6/WXG100 superfamily—and a new gram-positive secretion system? *Trends Microbiol.* **10**, 209–212
12. Gey Van Pittius, N. C., Gamielidien, J., Hide, W., Brown, G. D., Siezen, R. J., and Beyers, A. D. (2001) The ESAT-6 gene cluster of *Mycobacterium tuberculosis* and other high G+C gram-positive bacteria. *Genome Biol.* **2**, RESEARCH0044

13. Houben, E. N., Korotkov, K. V., and Bitter, W. (2014) Take five—type VII secretion systems of Mycobacteria. *Biochim. Biophys. Acta* **1843**, 1707–1716
14. Stanley, S. A., Raghavan, S., Hwang, W. W., and Cox, J. S. (2003) Acute infection and macrophage subversion by Mycobacterium tuberculosis require a specialized secretion system. *Proc. Natl. Acad. Sci. USA* **100**, 13001–13006
15. Siegrist, M. S., Unnikrishnan, M., McConnell, M. J., Borowsky, M., Cheng, T. Y., Siddiqi, N., Fortune, S. M., Moody, D. B., and Rubin, E. J. (2009) Mycobacterial ESX-3 is required for mycobactin-mediated iron acquisition. *Proc. Natl. Acad. Sci. USA* **106**, 18792–18797
16. Sayes, F., Sun, L., Di Luca, M., Simeone, R., Degaiffier, N., Fiette, L., Esin, S., Brosch, R., Bottai, D., Leclerc, C., and Majlessi, L. (2012) Strong immunogenicity and cross-reactivity of Mycobacterium tuberculosis ESX-5 type VII secretion: encoded PE-PPE proteins predicts vaccine potential. *Cell Host Microbe* **11**, 352–363
17. Bitter, W., Houben, E. N., Bottai, D., Brodin, P., Brown, E. J., Cox, J. S., Derbyshire, K., Fortune, S. M., Gao, L. Y., Liu, J., Geyvan Pittius, N. C., Pym, A. S., Rubin, E. J., Sherman, D. R., Cole, S. T., and Brosch, R. (2009) Systematic genetic nomenclature for type VII secretion systems. *PLoS Pathog.* **5**, e1000507
18. Houben, E. N., Besteiroer, J., Ummels, R., Wilson, L., Piersma, S. R., Jiménez, C. R., Ottenhoff, T. H., Luijck, J., and Bitter, W. (2012) Composition of the type VII secretion system membrane complex. *Mol. Microbiol.* **86**, 472–484
19. Hsu, T., Hingley-Wilson, S. M., Chen, B., Chen, M., Dai, A. Z., Morin, P. M., Marks, C. B., Padiyar, J., Goulding, C., Ginger, M., Eisenberg, D., Russell, R. G., Derrick, S. C., Collins, F. M., Morris, S. L., King, C. H., and Jacobs, W. R., Jr. (2003) The primary mechanism of attenuation of bacillus Calmette-Guérin is a loss of secreted lytic function required for invasion of lung interstitial tissue. *Proc. Natl. Acad. Sci. USA* **100**, 12420–12425
20. Coros, A., Callahan, B., Battaglioli, E., and Derbyshire, K. M. (2008) The specialized secretory apparatus ESX-1 is essential for DNA transfer in Mycobacterium smegmatis. *Mol. Microbiol.* **69**, 794–808
21. Daleke, M. H., Ummels, R., Bawono, P., Heringa, J., Vandenbroucke-Grauls, C. M., Luijck, J., and Bitter, W. (2012) General secretion signal for the mycobacterial type VII secretion pathway. *Proc. Natl. Acad. Sci. USA* **109**, 11342–11347
22. Ramsdell, T. L., Huppert, L. A., Sysoeva, T. A., Fortune, S. M., and Burton, B. M. (2015) Linked domain architectures allow for specialization of function in the FtsK/SpoIIIE ATPases of ESX secretion systems. *J. Mol. Biol.* **427**, 1119–1132
23. Brodin, P., Majlessi, L., Marsollier, L., de Jonge, M. I., Bottai, D., Demangel, C., Hinds, J., Neyrolles, O., Butcher, P. D., Leclerc, C., Cole, S. T., and Brosch, R. (2006) Dissection of ESAT-6 system 1 of Mycobacterium tuberculosis and impact on immunogenicity and virulence. *Infect. Immun.* **74**, 88–98
24. Das, C., Ghosh, T. S., and Mande, S. S. (2011) Computational analysis of the ESX-1 region of Mycobacterium tuberculosis: insights into the mechanism of type VII secretion system. *PLoS One* **6**, e27980
25. Li, H., Zhang, X., Bi, L., He, J., and Jiang, T. (2011) Determination of the crystal structure and active residues of FabV, the enoyl-ACP reductase from Xanthomonas oryzae. *PLoS One* **6**, e26743
26. Krogh, A., Larsson, B., von Heijne, G., and Sonnhammer, E. L. (2001) Predicting transmembrane protein topology with a hidden Markov model: application to complete genomes. *J. Mol. Biol.* **305**, 567–580
27. Buchan, D. W., Minneci, F., Nugent, T. C., Bryson, K., and Jones, D. T. (2013) Scalable web services for the PSIPRED Protein Analysis Workbench. *Nucleic Acids Res.* **41**, W349–57
28. Fernandez, D., Dang, T. A., Spudich, G. M., Zhou, X. R., Berger, B. R., and Christie, P. J. (1996) The Agrobacterium tumefaciens virB7 gene product, a proposed component of the T-complex transport apparatus, is a membrane-associated lipoprotein exposed at the periplasmic surface. *J. Bacteriol.* **178**, 3156–3167
29. Mawuenyega, K. G., Forst, C. V., Dobos, K. M., Belisle, J. T., Chen, J., Bradbury, E. M., Bradbury, A. R., and Chen, X. (2005) Mycobacterium tuberculosis functional network analysis by global subcellular protein profiling. *Mol. Biol. Cell* **16**, 396–404
30. Winans, S. C., Kerstetter, R. A., Ward, J. E., and Nester, E. W. (1989) A protein required for transcriptional regulation of Agrobacterium virulence genes spans the cytoplasmic membrane. *J. Bacteriol.* **171**, 1616–1622
31. Tao, J., Han, J., Wu, H., Hu, X., Deng, J., Fleming, J., Maxwell, A., Bi, L., and Mi, K. (2013) Mycobacterium fluoroquinolone resistance protein B, a novel small GTPase, is involved in the regulation of DNA gyrase and drug resistance. *Nucleic Acids Res.* **41**, 2370–2381
32. Leupold, C. M., Goody, R. S., and Wittinghofer, A. (1983) Stereochemistry of the elongation factor Tu X GTP complex. *Eurochem J. Biochem.* **135**, 237–241
33. Solomonson, M., Huesgen, P. F., Wasney, G. A., Watanabe, N., Gruninger, R. J., Prehna, G., Overall, C. M., and Strynadka, N. C. (2013) Structure of the mycosin-1 protease from the mycobacterial ESX-1 protein type VII secretion system. *J. Biol. Chem.* **288**, 17782–17790
34. Doublé, S. (2007) Production of selenomethionyl proteins in prokaryotic and eukaryotic expression systems. *Methods Mol. Biol.* **363**, 91–108
35. Adams, P. D., Grosse-Kunstleve, R. W., Hung, L. W., Ioerger, T. R., McCoy, A. J., Moriarty, N. W., Read, R. J., Sacchettini, J. C., Sauter, N. K., and Terwilliger, T. C. (2002) PHENIX: building new software for automated crystallographic structure determination. *Acta Crystallogr. D Biol. Crystallogr.* **58**, 1948–1954
36. Emsley, P., and Cowtan, K. (2004) Coot: model-building tools for molecular graphics. *Acta Crystallogr. D Biol. Crystallogr.* **60**, 2126–2132
37. Laskowski, R. A., MacArthur, M. W., Moss, D. S., and Thornton, J. M. (1993) Procheck—a program to check the stereochemical quality of protein structures. *J. Appl. Cryst.* **26**, 283–291
38. Duhovny, D., Nussinov, R., and Wolfson, H. J. (2002) Efficient unbound docking of rigid molecules. *Lect. Notes Comput. Sci.* **2452**, 185–200
39. Schneidman-Duhovny, D., Inbar, Y., Polak, V., Shatsky, M., Halperin, I., Benyamini, H., Barzilai, A., Dror, O., Haspel, N., Nussinov, R., and Wolfson, H. J. (2003) Taking geometry to its edge: fast unbound rigid (and hinge-bent) docking. *Proteins* **52**, 107–112
40. Luthra, A., Mahmood, A., Arora, A., and Ramachandran, P. (2008) Characterization of Rv3868, an essential hypothetical protein of the ESX-1 secretion system in Mycobacterium tuberculosis. *J. Biol. Chem.* **283**, 36532–36541
41. Sani, M., Houben, E. N. G., Geurtsen, J., Pierson, J., de Punder, K., van Zon, M., Wever, B., Piersma, S. R., Jiménez, C. R., Daffé, M., Appelmelk, B. J., Bitter, W., van der Wel, N., and Peters, P. J. (2010) Direct visualization by cryo-EM of the mycobacterial capsular layer: a labile structure containing ESX-1-secreted proteins. *PLoS Pathog.* **6**, e1000794
42. Brennan, P. J., and Nikaido, H. (1995) The envelope of mycobacteria. *Annu. Rev. Biochem.* **64**, 29–63
43. Fronzes, R., Christie, P. J., and Waksman, G. (2009) The structural biology of type IV secretion systems. *Nat. Rev. Microbiol.* **7**, 703–714
44. Korotkov, K. V., Sandkvist, M., and Hol, W. G. (2012) The type II secretion system: biogenesis, molecular architecture and mechanism. *Nat. Rev. Microbiol.* **10**, 336–351
45. Gomis-Rüth, F. X., Moncalián, G., Pérez-Luque, R., González, A., Cabezon, E., de la Cruz, F., and Coll, M. (2001) The bacterial conjugation protein TrwB resembles ring helicases and F1-ATPase. *Nature* **409**, 637–641

Received for publication January 26, 2015.

Accepted for publication July 27, 2015.